Origin of triangular island shape and double-step bunching during GaN growth by molecular-beam epitaxy under excess Ga conditions

M. H. Xie,[1,*] M. Gong,[1] E. K. Y. Pang,[1] H. S. Wu,[1] and S. Y. Tong[2]
[1]*Physics Department and the Joint Laboratory on New Materials, The University of Hong Kong, Pokfulam Road, Hong Kong*
[2]*Department of Physics and Materials Science, City University of Hong Kong, Tat Chee Avenue, Kowloon, Hong Kong*
(Received 31 October 2005; revised manuscript received 16 June 2006; published 22 August 2006)

GaN homoepitaxial growth by molecular-beam epitaxy under both excess gallium (Ga) and excess nitrogen (N) conditions is investigated. Based on two-dimensional island shape and surface step structures, we suggest the growth is kinetic-limited under the excess-Ga condition but diffusion-limited in the excess-N regime. The triangular GaN islands and double step bunching seen on surfaces prepared under excess-Ga are attributed to a difference in adatom attachment and/or site exchange rates between *A* and *B* steps, which is induced by surfactant Ga adlayers on GaN(0001).

DOI: 10.1103/PhysRevB.74.085314 PACS number(s): 68.55.Jk, 68.35.Bs, 68.35.Fx

I. INTRODUCTION

Progress in III-nitrides in the past decades has been tremendous, especially in the areas of material growth and device applications.[1,2] Accompanied with such technological advancements, knowledge of surface structure and film growth kinetics of nitride films is also gained. For example, it was realized based on both experimental and theoretical studies that layers of gallium (Ga) atoms would wet the surface of a growing film when a Ga-rich flux was used during molecular-beam epitaxy (MBE).[3–6] These excess-Ga adlayers in turn affected the kinetics of adatom diffusion[7,8] and island nucleation.[9,10] On a bare GaN(0001) surface, the energy barrier for nitrogen (N) adatom diffusion was $\sim$1.5 eV according to density-functional theory calculations,[7] whereas it was reduced to about 0.5 eV when diffusing along a path underneath the surface excess metal adlayers.[8] The consequent enhancement of adatom diffusion would then give rise to smoother and better quality epi-films, which were consistent with experimental observations.[11,12] On the other hand, the surfactant effect of surface metallic adlayers also changed island nucleation kinetics, and the experimentally observed GaN "ghost" islands were seen to be directly related to surface Ga adlayers.[9,10] The epitaxial growth mode could also be changed by surfactant Ga when deposited on some foreign substrates such as aluminum nitride.[13]

In an earlier study of GaN homoepitaxy by MBE under excess-Ga fluxes, triangular island shape and double step bunching were observed.[14] Such morphological features suggested anisotropic growth rates of surface steps, the kinetic origin of which was not fully known. In this paper, we compare GaN growth under Ga-rich versus N-rich conditions of MBE and reveal different rate-limiting kinetics for different deposition conditions. The kinetics leading to the triangular island shape and double step bunching under excess Ga is then examined. Using kinetic Monte Carlo (kMC) simulations, factors such as adatom diffusivity and corner-crossing, the energy barriers for adatom attachment at steps, and the barriers for exchanging sites between atoms of the deposit and surfactant Ga are all investigated.

II. EXPERIMENTS

Molecular-beam epitaxy of GaN films and subsequent surface examinations by scanning tunneling microscopy (STM) were conducted in a multichamber ultrahigh vacuum (UHV) system, where the MBE reactor and the UHV-STM chamber were connected via vacuum interlocks.[15] The MBE chamber was equipped with conventional effusion cells for Ga and other group III metals plus a radiofrequency plasma unit for N source. The MBE chamber also contained the facility of reflection high-energy electron diffraction (RHEED), allowing *in situ* observations of growing surfaces in real time. The base pressures of both MBE and STM chambers were below 2×10^{-10} torr. However, in the MBE chamber, the pressure increased to 5×10^{-5} torr during film deposition at a N_2 flow rate of 0.13 standard cubic centimeters per minute. Typical deposition rate of GaN was 0.1 bilayers per second (BLs/s) as measured by the RHEED intensity oscillation.[15]

Nominally flat 6*H*-SiC(0001) wafers (Cree) were used as the substrate for GaN deposition. They were diced into 11×4 mm^2 rectangular pieces and cleaned consecutively in acetone, alcohol, and deionized water before being loaded into UHV chambers. After a degassing procedure in vacuum overnight at $\sim$400 °C, the substrates were deoxidized at $\geqslant$1000 °C under a flux of silicon until sharp $(\sqrt{3}\times\sqrt{3})R30°$ diffraction patterns were obtained as seen by low-energy electron diffraction (LEED). They were then transferred to the MBE chamber, where thick ($\sim$0.5 μm) GaN buffer layers were grown at 650 °C. The III/V flux ratio for GaN buffer layer deposition was $\sim$2, which led to relatively flat surfaces and the Ga polarity of the films.[15] The latter assignment for the film's polarity was made based on surface reconstruction observations by RHEED at different temperatures and different Ga coverage.[3–5] For some samples, they were immediately cooled upon the completion of buffer layer deposition to temperatures below 500 °C, while for others an annealing procedure was adopted prior to sample cooling. The films prepared using excess-Ga fluxes contained excess Ga adlayers on surface,[3–6] whereas for those undergoing the annealing procedure, Ga adlayers were desorbed and there was no excess Ga on the surface.

Island nucleation experiments were conducted on both Ga-adlayer covered and bare GaN(0001) surfaces at $\leqslant$500 °C. It was done by depositing a submonolayer material (e.g., $\sim$0.3 BLs) on the buffer layer surface, where the

 ©2006 The American Physical Society

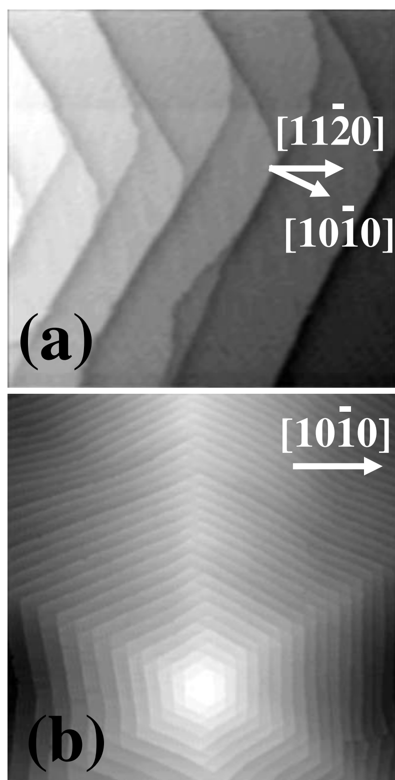

FIG. 1. STM images showing (a) a GaN buffer layer surface following deposition under excess Ga flux conditions, revealing the particular step structure of the surface (image size 100 nm $\times$ 100 nm), and (b) a similar surface viewed in a large length scale, depicting the spiral mound caused by growth at threading screw dislocations (image size: 1500 nm $\times$ 1500 nm).

low substrate temperature ensured the nucleation growth mode due to reduced diffusion length of adatoms. Having completed the submonolayer deposition, the samples were thermally quenched by switching off the heating current flowing through the long side of the rectangular sample pieces. They were then examined by STM at room temperature at a tunneling current of 0.1 nA and sample bias of −2.5 V.

III. RESULTS

Figure 1(a) shows an example of the buffer layer surface prepared using an excess-Ga flux. It depicts the relative smoothness of the surface as well as the particular features of surface steps on GaN(0001). On a large length scale, however, the surface is composed of spiral mounds due to preferential growth at threading screw dislocations.[16] The density and size of the spiral mounds depend on the initial substrate surface condition as well as the growth parameters used for initial stage buffer film growth. An example of a well developed spiral mound is shown in Fig. 1(b). Such spiral mounds show hexagonal shape in their bases, reflecting the lattice symmetry of wurtzite phase GaN on its (0001) plane. From Fig. 1, one may also note that the steps are two bilayers high running perpendicular to $\langle 10\bar{1}0\rangle$ directions, i.e., there is a double bilayer step bunching. Perpendicular to $\langle 11\bar{2}0\rangle$, however, one observes debunched steps. As explained in Ref. 14, such step features are characteristic of a wurtzite crystal surface. Another observation from Fig. 1(b) is the curved steps far from the mound top but straight steps near the mound top.

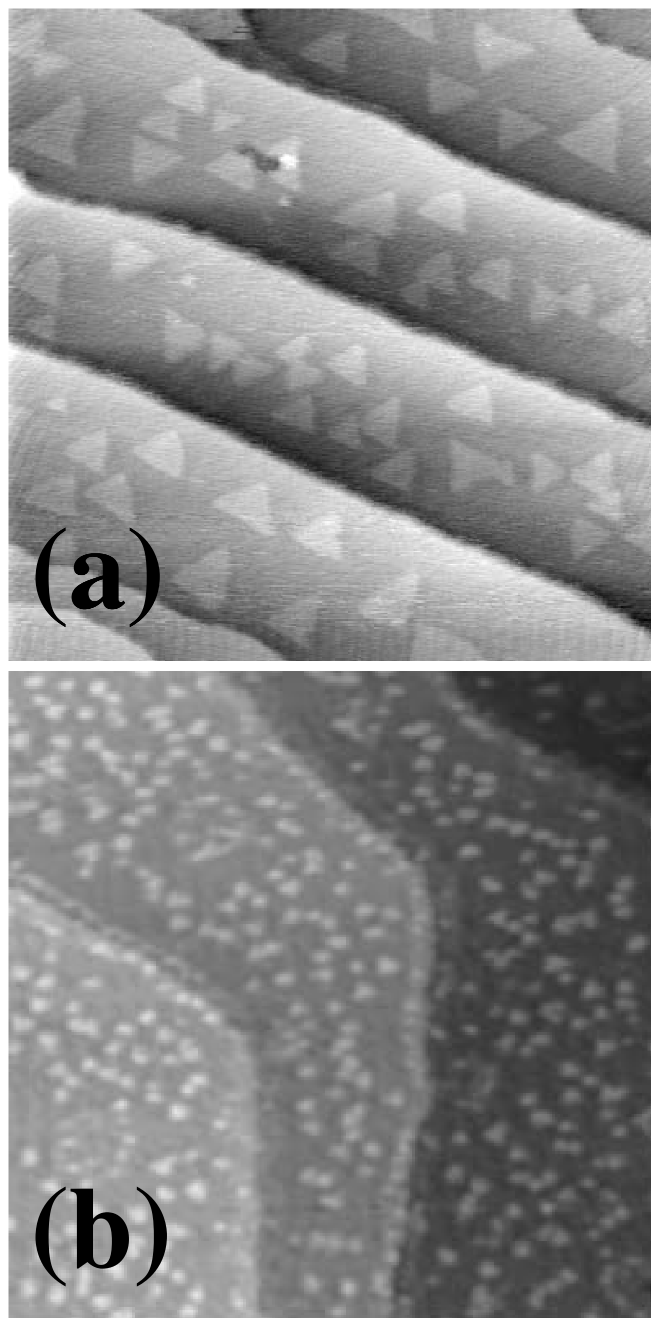

FIG. 2. STM images of surfaces following ~0.3 BLs GaN deposition at $\leq$500 °C on (a) a GaN(0001) surface covered with excess-Ga adlayers (image size: 200 nm $\times$ 200 nm) and (b) a bare GaN surface without the excess Ga adlayer (image size: 300 nm $\times$ 300 nm).

Figure 2(a) shows a GaN surface following a submonolayer material deposition on the buffer layer surface at low temperature using an excess-Ga flux, while Fig. 2(b) shows a

similar surface prepared on a bare GaN(0001) and using an excess N flux. Comparing the two, one observes that the island density, size, and shape are all different. In Fig. 2(a), islands are relatively large but low in density, showing distinct triangular shape. On the other hand, islands in Fig. 2(b) are noticeably small but with a higher density. The shape of the latter islands is more circular. Line profiles across the islands reveal they are one bilayer high and so they are all two-dimensional islands. It should be mentioned, however, that for islands in Fig. 2(a), they were mostly converted from "ghost" islands by continuous STM imaging, which was detailed in Refs. 9 and 10.

IV. DISCUSSIONS

A. Diffusion versus kinetic limited growth

The differences between the two surfaces shown in Figs. 2(a) and 2(b) obviously reflect different kinetics governing the growth of GaN films under different flux and surface conditions. Recent theoretical studies have revealed a significant change in surface diffusion kinetics on excess-metal covered GaN(0001) from that on a bare surface.[8] A much lower energy barrier for diffusion was found when excess metal adlayers were present. The existence of excess Ga adlayers may also change the characteristics of surface steps, affecting adatom attachment rates at steps. For growth on bare surfaces, the high-energy barrier for diffusion leads to high densities of nucleation islands, while limited edge diffusion of atoms along the peripheries of islands makes the island edges rough and less distinct in shape. The result of Fig. 2(b) seems to conform to such expectations. In fact, under such growth conditions, adatom incorporation at steps readily occurs. The comparatively slower rate of adatom surface diffusion than that of attachment at steps makes GaN growth on its bare surface diffusion-rate-limited.[17] In this diffusion-limited regime, the difference in reactivity of surface steps will not become manifest. The attachment rates of adatoms at different steps, though they may differ, will all be quicker than that of adatom transport to steps by diffusion, so the step growth rate becomes determined by surface diffusion and is isotropic.

Under Ga-rich fluxes and when the surface is covered by excess Ga adlayers, the energy barrier for diffusion is significantly reduced,[8] so fewer islands are nucleated. Further, excess Ga atoms on the surface may decorate steps, passivating the dangling bonds of edge atoms, so adatom attachment and incorporation at those steps becomes difficult. It requires overcoming additional energy barriers to displace these step-decorating atoms,[18] so the rate will become slower. The reduced rates of attachment at steps compared with the increased rate of diffusion on terrace makes the growth kinetic-limited.[17] In this latter growth regime, any difference between steps in their kinetic coefficients will lead to anisotropic step growth rates and thus to step bunching and triangular island shape, as seen by experiments.

For the kinetic-limited growth regime, there exist different surface processes that may give rise to similar island shape selection and/or step bunching. In the following, we shall examine each individual process and identify the most relevant kinetics governing GaN growth by MBE under excess Ga.

B. Kinetics leading to triangular island shape and double step bunching

1. Adatom diffusivity, corner crossing, and detachment

As detailed in a previous paper,[14] there are two types of steps on a GaN(0001) surface: a type-*A* step which has two dangling bonds per edge atom, and a type-*B* step, where there is only one dangling bond per edge atom. The two steps alternate upon turning 60° on the same surface or upon descending a single or odd number of bilayer steps.[14] One apparent consequence of such a bonding characteristics is the difference in binding energy between the two steps. For an atom to detach from an *A* step, more chemical bonds need to be broken, the rate of which will be noticeably smaller than that for detachment from a *B* step. If not for detachment, adatom diffusion along the step edges would also show different rates between the two steps. There can further be an asymmetry in corner crossing of edge atoms when diffusing from *A* to *B* versus that from *B* to *A* steps. All of these may result in different atom fluxes to different steps and thus the anisotropic growth rates of the step.

Unlike the case of GaN growth under excess N, significant edge diffusion and corner crossing of atoms when deposited under excess Ga can be apparent from the compact islands in Fig. 2(a). Otherwise, less distinct or dendritic islands would have resulted.[19] Adatom edge diffusion is further evident from the curved steps constituting the spiral mound in Fig. 1(b). Due to the point effect of island (mound) edges, more atoms are captured by the corners of the mound, which then diffuse away toward the centers of steps.[19] If the length of a step is longer than twice the diffusion length of edge atoms, the initial straight step edge may not be maintained but a curvature will develop. In Fig. 1(b), straight steps are seen near the top of the spiral mound, where the steps are short, whereas curved steps are seen away from the mound top where they are longer. By measuring the length of the step at which it starts to develop curvature, one may provide a rough estimate of the edge diffusion length.

Some previous studies have shown, however, that adatom edge diffusivity is not quite relevant to step growth rate.[20,21] On the one hand, a low diffusion rate of atoms along steps will result in high kink densities and thus promote incorporation of atoms at such steps. On the other hand, the low diffusivity of atoms also means it takes longer for adatoms to find the kinks. The two factors counterbalance each other, therefore edge atom diffusivity will not have much influence on step growth rate.[21] Subsequent studies of the problem revealed that the asymmetry of adatom corner crossing might be more relevant.[22] For example, a lower rate of adatom transport from *A* to *B* by corner crossing than that from *B* to *A* will generate a net atom flux from *B* to *A*, leading to a high growth rate of *A* steps. Asymmetric corner crossing was shown to account for the shape selection of Pt islands on its (111) surface.[22] For GaN growth concerned here, however, in addition to triangular islands, double step bunching is consistently observed in the step-flow growth regime (see, for

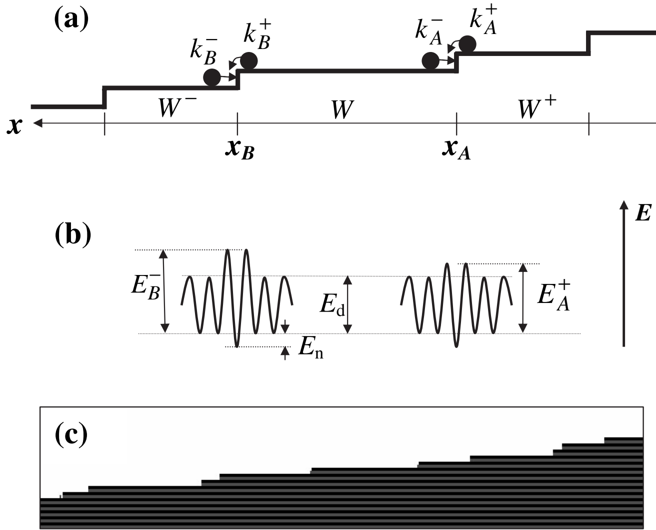

FIG. 3. Schematic diagram showing in one dimension a vicinal surface (a) and the associated energy landscape near steps (b). A simulated surface after growth of 100 layers is shown in (c), where it is assumed that E_d=1.0 eV, the binding energy E_n=1.0 eV, $E_A^{\pm}$=1.2 eV, and $E_B^{\pm}$=1.3 eV. The temperature is 950 K and the deposition rate is 0.1 layers per second. The dark and gray colors mark the A and B steps, respectively.

example, Fig. 1 and those found during vicinal surface growth[16]). As for the latter, corners are rare in the length scale of adatom diffusion and the steps are at different levels for growth of vicinal surfaces, yet they grow at different rates causing the step bunching. Asymmetry of edge atom corner crossing cannot be the dominant factor here.

Another possible cause for island shape selection and step bunching is the rate of atom detachment from steps. If these rates are different for different steps, subsequent recapture of the detached atoms by all steps naturally generates a net flux from one step to another, giving rise to the anisotropic growth rates. As some earlier works showed, such a factor indeed resulted in island shape transition from initial hexagons to triangles.[20] For growth of vicinal surfaces in the step-flow regimes, our kMC simulations also produced double step bunching.[23] However, in order to produce such growth features, the temperature of deposition has to be high so that atom detachment is significant. For GaN, the chemical bonds are quite strong [~2.1 eV (Ref. 24)], so it is highly questionable whether atom detachment is active at the temperatures of our experiments [$T\leq 500$ °C for Fig. 2(a) and $T\sim 650$ °C for Fig. 1]. We thus may also rule out its relevance to GaN growth considered here.

2. Energy barriers at steps

For growth of long steps and at moderate temperatures, neither corner crossing nor atom detachment is relevant. So we ought to seek some other causes for the observed growth phenomena of GaN under excess Ga. In this subsection, we examine the effect of step-edge barriers. Specifically, consider growth of a vicinal surface of Fig. 3(a). The step growth rates may be expressed as

$$\frac{\partial x_{A,B}}{\partial t} = \beta^+_{A,B}(n^+_{A,B} - n^0_{A,B}) + \beta^-_{A,B}(n^-_{A,B} - n^0_{A,B}), \quad (1)$$

where t is the deposition time and $x_{A,B}$ are positions of A or B steps. $\beta^{\pm}$ represent step kinetic coefficients expressing the effectiveness of a step to capture adatoms from its upper (+) or lower (−) terraces. $n^{\pm}$ is the adatom concentration in the vicinity of a step during deposition while n^0 is that at equilibrium. The above one-dimensional expression obviously neglects the lateral fluctuations of steps, which may be justifiable for straight steps. Under the condition of local mass transport, i.e., when adatoms are confined within an individual terrace bounded by nontransparent steps,[25,26] one may solve for n and find the step growth rate to be[27–29]

$$\frac{\partial x_A}{\partial t} = k_A^- W + k_A^+ W^+, \quad (2)$$

$$\frac{\partial x_B}{\partial t} = k_B^- W^- + k_B^+ W, \quad (3)$$

where constants k's are proportional to β's, and W's are the terrace widths.[29] Subtracting the above two equations, noting that $W=x_B-x_A\approx 0$ when double step bunching has occurred and $W^+\approx W^-$ [statistically these two terraces are equivalent, see Fig. 3(a)], one has[30]

$$\frac{\partial W}{\partial t} \propto k_B^- - k_A^+. \quad (4)$$

In order to promote and maintain double step bunching during growth, one obviously requires $\frac{\partial W}{\partial t}\leq 0$, which means that $k_B^-\leq k_A^+$. In other words, adatom capture by a B step from its lower terrace has to be no more efficient than that for an A step to capture adatoms from its upper terrace.[30]

To satisfy the above condition, we may let E_B^-, the energy barrier for a B step to capture adatoms from its lower terrace, be greater than E_A^+, the barrier for an A step to capture adatoms from its upper terrace [see Fig. 3(b)]. A number of surface energy profiles may be devised to conform to the above condition. However, we first rule out those where E_B^- and E_A^+ are both smaller than E_d, the barrier for adatom diffusion on terraces. This is because such energy profiles will make growth diffusion-limited. In other words, the smaller $E_{A,B}^-$ and $E_{A,B}^+$ make adatom attachment to steps quick processes, and the step growth rate becomes limited by adatom transportation to steps by diffusion. As noted earlier, under such a circumstance, the difference in step kinetic coefficients between A and B may not manifest and step growth rate is isotropic. Another set of energy landscapes that we can also rule out is for cases in which $E_A^-\neq E_A^+$ and $E_B^-\neq E_B^+$, otherwise it creates the so called Ehrlich-Schwoebel barriers at steps.[31] The existence of such energy barriers will either create growth instability leading to multistep bunching or oppositely stabilize growth giving rise to unbunched step structures.[29] Experimentally, we always observe double step bunching while multistep bunching is observed only under special occasions.[32] Having ruled out all those mentioned above, we are left with only an energy profile as shown in Fig. 3(b), where $E_A^-=E_A^+$ and $E_B^-=E_B^+$ and that $E_A<E_B$. Note

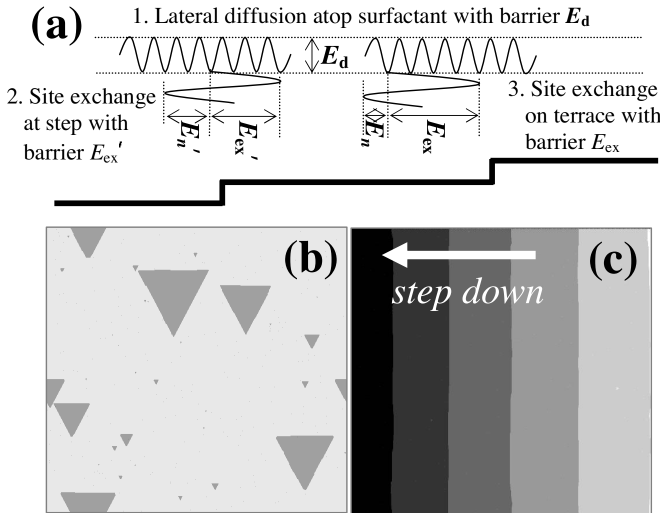

FIG. 4. (a) A schematic of the surface energy diagram dictating (1) adatom diffusion on a surfactant layer and for site exchange with surfactant atoms at (2) steps or (3) on terraces. (b) A simulated surface following 0.2 ML material deposition on a flat surface. (c) A simulated vicinal surface following 10 ML deposition. In simulation, it was assumed that the rates of exchange on a flat terrace R_{ex}, at A steps R_{ex}^A and at B steps R_{ex}^B, followed a relation $R_{ex}:R_{ex}^A:R_{ex}^B=1:50:50^2$ (which translated into an energy difference between E_{ex} and $E'_{A,ex}$ or between $E'_{A,ex}$ and $E'_{B,ex}$ of about $3.9kT$). Size of (b) and (c): 600×600 sites.

that both E_A and E_B are greater than E_d and that $E_n \gg 0$ ensure the local mass transport kinetics considered here. KMC simulations of growth of such surfaces indeed produced double step bunching in the step-flow growth regime and triangular island shape in the nucleation regime. An example of the simulated vicinal surface in 1+1 dimension is shown in Fig. 3(c).

Physically, the higher-energy barriers at steps can be created by surface excess Ga adatoms decorating the steps. For a diffusing N atom to attach to the step, it needs to displace the step-decorating Ga through a site-exchange process, which costs additional energy.[28] The difference between A and B steps may originate from the difference in the number of bonds it needs to break when displacing Ga.[14]

3. Exchange barriers

The precise nature of steps as affected by excess Ga is not fully known at the moment. The assumption made above of high-energy barriers at steps as caused by surface excess Ga is thus speculative. There can be another scenario where adatom incorporation at steps as well as on terraces both involve the site-exchange process as proposed for surfactant mediated growth,[33] and the surfactant makes adatom surface diffusion global. Figure 4(a) shows a schematic energy profile for the case in which adatom diffusion on top of the surfactant layer is dictated by the energy barrier E_d, while atom site exchange on the terrace or at step sites is determined by the barriers E_{ex} and E'_{ex}, respectively. Generally, adatoms diffuse rapidly atop the surfactant layer (or within the excess Ga adlayer[8]) with a smaller E_d. During diffusion, adatoms attempt to exchange sites with surfactant atoms on terrace by surmounting the energy barrier E_{ex} and become buried underneath the surfactant, which acts as the nuclei for island growth, or they exchange sites at the peripheries of islands or step edges by overcoming the barrier $E'_{ex}<E_{ex}$ (the so called aided exchange) and become trapped by steps.[33] As is shown, this kinetics is different from that considered in the previous subsection, as now the surface has become globally accessible by adatoms and the steps are transparent.[25,26] Adatoms diffuse a long distance, crossing many steps, before accomplishing the site-exchange event and becoming incorporated in film. In this latter case, adatom concentration n will be fairly constant across the whole surface, and so, according to Eq. (1), the step growth rate is directly related to the step kinetic coefficient β. If they are different between A and B steps, anisotropic growth rates of these steps can be expected.

Step kinetic coefficients β are primarily determined by the energy barriers at steps, including E'_{ex} introduced here. If E'_{ex} at step A and B differ, the growth rates of A and B steps will be different, giving rise to the triangular island shape and double step bunching on a wurtzite crystal surface. Figures 4(b) and 4(c) show simulated surfaces in 2+1 dimensions following deposition on flat and vicinal *hcp* surfaces, respectively, revealing the expected island shape and the doubly bunched step structures.

Finally, it is noted that both kinetics of local adatom transport considered in Sec. IV B 2 and that of global adatom transport studied in this subsection result in the same growth phenomena of triangular island shape and double step bunching. Thus, based on such morphological features alone, one may not distinguish the two. Nevertheless, to account for the larger E_A and E_B in Sec. IV B 2 and the E'_{ex} in this subsection, we have invoked the same site-exchange process for adatom step incorporation. If such a site-exchange process is indeed involved during MBE of nitride films under excess Ga, in the island nucleation regime, one expects to observe a characteristic island size distribution that shows no peak according to theoretical predictions.[34,35] We thus have exam-

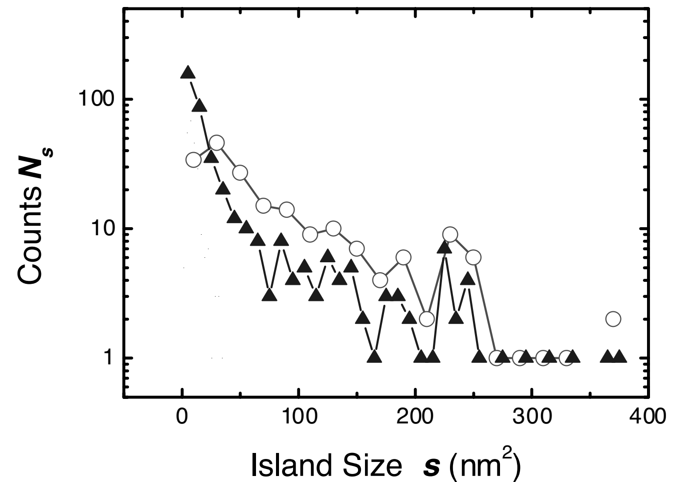

FIG. 5. Island size distribution curves for two independent sets of data prepared under similar excess Ga conditions (III/V ~2) and at 420 °C.

ined many such islands and their size distributions are given in Fig. 5 (see also Fig. 3 of Ref. 9). The distribution curves of two independent sets of data show no clear peaks, suggesting that nitride growth under excess Ga may indeed be surfactant mediated, involving the site-exchange processes. As for the question of whether adatom diffusion is local or global, however, the available experimental data are not sufficient to distinguish the two; further studies are needed in this regard.

V. SUMMARY AND CONCLUSIONS

Different morphologies of GaN are observed during growth by MBE under excess-Ga and excess-N conditions. The presence of Ga adlayers on surface changes the growth from diffusion-limited to kinetic-limited regimes, and the growth phenomena of triangular island shape and double step bunching are seen only under excess Ga conditions. The very kinetics leading to anisotropic growth rates of surface steps is the different energy barriers for adatom incorporation at *A* versus *B* steps and/or for site exchange between atoms of the deposit and surfactant Ga. The surfactant Ga adlayer makes adatom diffusion faster and yet its incorporation at step difficult.

ACKNOWLEDGMENTS

This work is supported by grants from the Research Grants Council of the Hong Kong Special Administrative Region, China (Project No. HKU7035/03P).

---

*Email address: mhxie@hkusua.hku.hk

[1] S. Nakamura and G. Fasol, *The Blue Laser Diode, GaN Based Light Emitters and Lasers* (Springer, Berlin, 1997).

[2] *Gallium Nitride I*, edited by J. I. Pankove and T. D. Moustakas, Semiconductors and Semimetals Vol. 50 (Academic, New York, 1998); *Gallium Nitride II*, edited by J. I. Pankove and T. D. Moustakas, Semiconductors and Semimetals Vol. 57 (Academic, New York, 1999).

[3] A. R. Smith, R. M. Feenstra, D. W. Greve, J. Neugebauer, and J. E. Northrup, Phys. Rev. Lett. **79**, 3934 (1997).

[4] A. R. Smith, R. M. Feenstra, D. W. Greve, M.-S. Shin, M. Skowronski, J. Neugebauer, and J. E. Northrup, Appl. Phys. Lett. **72**, 2114 (1998).

[5] A. R. Smith, R. M. Feenstra, D. W. Greve, M.-S. Shin, M. Skowronski, J. Neugebauer, and J. E. Northrup, J. Vac. Sci. Technol. B **16**, 2242 (1998).

[6] S. H. Xu, Huasheng Wu, X. Q. Dai, W. P. Lau, L. X. Zheng, M. H. Xie, and S. Y. Tong, Phys. Rev. B **67**, 125409 (2003).

[7] T. K. Zywietz, J. Neugebauer, and M. Scheffler, Appl. Phys. Lett. **73**, 487 (1998).

[8] J. Neugebauer, T. K. Zywietz, M. Scheffler, J. E. Northrup, H. Chen, and R. M. Feenstra, Phys. Rev. Lett. **90**, 056101 (2003).

[9] M. H. Xie, L. X. Zheng, X. Q. Dai, H. S. Wu, and S. Y. Tong, Surf. Sci. **558**, 195 (2004).

[10] L. X. Zheng, M. H. Xie, S. M. Seutter, S. H. Cheung, and S. Y. Tong, Phys. Rev. Lett. **85**, 2352 (2000).

[11] E. J. Tarsa, B. Heying, X. H. Wu, P. Fini, S. P. DenBaars, and J. S. Speck, J. Appl. Phys. **82**, 5472 (1997).

[12] R. M. Feenstra, Huajie Chen, V. Ramachandran, C. D. Lee, A. R. Smith, J. E. Northrup, T. Zywietz, J. Neugebauer, and D. W. Greve, Surf. Rev. Lett. **7**, 601 (2000).

[13] G. Mula, C. Adelmann, S. Moehl, J. Oullier, and B. Daudin, Phys. Rev. B **64**, 195406 (2001).

[14] M. H. Xie, S. M. Seutter, W. K. Zhu, L. X. Zheng, H. S. Wu, and S. Y. Tong, Phys. Rev. Lett. **82**, 2749 (1999).

[15] S. M. Seutter, M. H. Xie, W. K. Zhu, L. X. Zheng, H. S. Wu, and S. Y. Tong, Surf. Sci. **445**, L71 (2000).

[16] M. H. Xie, L. X. Zheng, S. H. Cheung, Y. F. Ng, Huasheng Wu, S. Y. Tong, and N. Ohtani, Appl. Phys. Lett. **77**, 1105 (2000).

[17] Ivan V. Markov, *Crystal Growth for Beginners, Fundamentals of Nucleation, Crystal Growth and Epitaxy*, 2nd ed. (World Scientific, Singapore, 2003).

[18] D. Kandel, Phys. Rev. Lett. **78**, 499 (1997).

[19] T. Michely and J. Krug, *Islands, Mounds and Atoms, Patterns and Processes in Crystal Growth far from Equilibrium* (Springer, Berlin, 2004).

[20] S. Ovesson, A. Bogicevic, and B. I. Lundqvist, Phys. Rev. Lett. **83**, 2608 (1999).

[21] J. Jacobsen, K. W. Jacobsen, and J. K. Norskov, Surf. Sci. **359**, 37 (1996).

[22] J. Wu, E. G. Wang, K. Varga, B.-G. Liu, S. T. Pantelides, and Z. Zhang, Phys. Rev. Lett. **89**, 146103 (2002).

[23] M. Gong and M. H. Xie (unpublished).

[24] J. E. Northrup and J. Neugebauer, Phys. Rev. B **53**, 10477 (1996).

[25] S. Stoyanov and V. Tonchev, Phys. Rev. B **58**, 1590 (1998).

[26] Da-Jiang Liu, Elain S. Fu, M. D. Johnson, John D. Weeks, and Ellen D. Williams, J. Vac. Sci. Technol. B **14**, 2799 (1996).

[27] P. Bennema and G. H. Gilmer, in *Crystal Growth: An Introduction*, edited by P. Hartman (North-Holland, Amsterdam, 1973).

[28] D. Kandel and J. D. Weeks, Phys. Rev. Lett. **74**, 3632 (1995).

[29] M. H. Xie, S. Y. Leung, and S. Y. Tong, Surf. Sci. **515**, L459 (2002).

[30] M. H. Xie, S. M. Seutter, L. X. Zheng, S. H. Cheung, Y. F. Ng, H. S. Wu, and S. Y. Tong, MRS Internet J. Nitride Semiconductor Research, **5S1**, W3.29 (2000).

[31] R. L. Schwoebel and E. J. Shipsey, J. Appl. Phys. **37**, 3682 (1966); R. L. Schwoebel, *ibid.* **40**, 614 (1969); G. Ehrlich, and F. G. Hudda, J. Chem. Phys. **44**, 1039 (1966).

[32] M. H. Xie, S. H. Cheung, L. X. Zheng, Y. F. Ng, Huasheng Wu, N. Ohtani, and S. Y. Tong, Phys. Rev. B **61**, 9983 (2000).

[33] B.-G. Liu, J. Wu, E. G. Wang, and Z. Zhang, Phys. Rev. Lett. **83**, 1195 (1999).

[34] J. G. Amar and F. Family, Phys. Rev. Lett. **74**, 2066 (1995).

[35] A. Zangwill and E. Kaxiras, Surf. Sci. **326**, L483 (1995).